
Deep Learning of Preconditioners for Conjugate Gradient Solvers in Urban Water Related Problems

Johannes Sappl*

Unit of Environmental Engineering
 Faculty of Engineering Sciences
 Universität Innsbruck
 Technikerstraße 13, 6020 Innsbruck
 Austria
 johannes.sappl@uibk.ac.at

Laurent Seiler

Unit of Environmental Engineering
 Faculty of Engineering Sciences
 Universität Innsbruck
 Technikerstraße 13, 6020 Innsbruck
 Austria
 laurent.seiler@uibk.ac.at,

Matthias Harders

Interactive Graphics and Simulation Group
 Department of Computer Science
 Universität Innsbruck
 Technikerstraße 21 A, 6020 Innsbruck
 Austria
 matthias.harders@uibk.ac.at

Wolfgang Rauch

Unit of Environmental Engineering
 Faculty of Engineering Sciences
 Universität Innsbruck
 Technikerstraße 13, 6020 Innsbruck
 Austria
 wolfgang.rauch@uibk.ac.at,

Abstract

Solving systems of linear equations is a problem occurring frequently in water engineering applications. Usually the size of the problem is too large to be solved via direct factorization. One can resort to iterative approaches, in particular the conjugate gradients method if the matrix is symmetric positive definite. Preconditioners further enhance the rate of convergence but hitherto only handcrafted ones requiring expert knowledge have been used. We propose an innovative approach employing Machine Learning, in particular a Convolutional Neural Network, to unassistedly design preconditioning matrices specifically for the problem at hand. Based on an in-depth case study in fluid simulation we are able to show that our learned preconditioner is able to improve the convergence rate even beyond well established methods like incomplete Cholesky factorization or Algebraic MultiGrid.

1 Introduction

Given $\mathbf{A} \in \mathbb{R}^{m \times n}$, $\mathbf{b} \in \mathbb{R}^m$ for some positive $m, n \in \mathbb{N}$ a system of m linear equations with n variables can be written as

$$\mathbf{Ax} = \mathbf{b}, \quad (1)$$

where $\mathbf{x} \in \mathbb{R}^n$ denotes some yet unknown solution. This type of problem frequently appears in urban water engineering and management applications, e. g., when solving an optimization problem using the method of least squares. We are particularly interested in linear systems (1) where $\mathbf{A} \in \mathbb{R}^{n \times n}$ is Symmetric Positive Definite (SPD) as well as sparse. Examples are finite-difference methods for space-time discretization of a Partial Differential Equation (PDE) in storm water modeling or computing flow continuity and head loss equations characterizing the hydraulic state of a pipe network as, e. g., in the software EPANET 2 (Rossman, 2000). Very often n can be quite large with millions or even billions of unknowns to solve for. In this case direct methods like Cholesky decomposition become infeasible since they scale poorly with the size of the underlying problem in terms of operations and memory needed (Benzi, 2002).

*corresponding author

Iterative approaches which improve approximate solutions based on previous estimates provide a remedy for this, albeit at the expense of accuracy. One of the best known iterative methods for solving sparse SPD systems is the Conjugate Gradient (CG) algorithm to which the following well-known a priori error bound applies. Let \mathbf{x}_j be the approximate solution obtained after the j -th CG-iteration, then the norm of the error depending on \mathbf{A} is limited by

$$\|\mathbf{x} - \mathbf{x}_j\|_{\mathbf{A}} \leq 2 \left[\frac{\sqrt{\kappa(\mathbf{A})} - 1}{\sqrt{\kappa(\mathbf{A})} + 1} \right]^j \|\mathbf{x} - \mathbf{x}_0\|_{\mathbf{A}}, \quad (2)$$

for some initial guess \mathbf{x}_0 (Saad, 2003), where the so-called condition number of \mathbf{A} is defined as

$$\kappa(\mathbf{A}) := \frac{\sigma_{\max}(\mathbf{A})}{\sigma_{\min}(\mathbf{A})} \geq 1, \quad (3)$$

and $\sigma_{\max}(\mathbf{A})$, $\sigma_{\min}(\mathbf{A})$ denote the maximum and minimum singular value of \mathbf{A} , respectively. If $\kappa(\mathbf{A}) \gg 1$ then problem (1) is said to be ill-conditioned since, as stated in (2), the asymptotic behavior of $\|\mathbf{x} - \mathbf{x}_j\|_{\mathbf{A}}$ is determined by $(1 + \varepsilon)^{-j}$ for some small $\varepsilon > 0$ as j approaches infinity. Based on (2) the rate of convergence of CG can be improved through preconditioning, e. g., from the right, via transforming (1) into another linear system with more favorable properties by means of some non-singular SPD matrix \mathbf{M} according to

$$\mathbf{A}\mathbf{M}^{-1}\mathbf{y} = \mathbf{b}, \quad \mathbf{x} = \mathbf{M}^{-1}\mathbf{y}, \quad (4)$$

since the solution \mathbf{x} to (1) coincides with the one to (4). The so-called preconditioner \mathbf{M} is chosen s. t. it is cheap to construct, apply, and furthermore $1 \leq \kappa(\mathbf{A}\mathbf{M}^{-1}) \ll \kappa(\mathbf{A})$, ultimately resulting in faster convergence of the Preconditioned Conjugate Gradient (PCG) method in agreement with (2). Note that one can also precondition (1) from the left $\mathbf{M}^{-1}\mathbf{A}$ or even perform split preconditioning $\mathbf{M}_1^{-1}\mathbf{A}\mathbf{M}_2^{-1}$, but since the eigenvalues of the respective matrices are equal, the rate of convergence of PCG is going to stay the same. Thus, without loss of generality we are committing ourselves to right preconditioning purely for implementation reasons in the remainder of this paper.

Good designs for the matrix \mathbf{M} require problem-specific knowledge and are often very situational meaning small changes to the system (1) can render \mathbf{M} inefficient. Instead of manually designing a new preconditioner each time the underlying problem changes, we propose taking advantage of a novel Machine Learning (ML) approach. Perhaps most related to this is a data-driven multigrid method optimizing restriction and prolongation operators for solving discretized PDEs (Katrutsa et al., 2017).

2 Methods

At the heart of ML is a data set $(x_j, y_j)_j$ and a model f with internal parameters that have to be adjusted based on the data s. t. $f(x_j) =: \hat{y}_j$ has small loss $\ell(\hat{y}_j, y_j)$ for as many samples j as possible. If the ground truths y_j are not available the problem is called unsupervised and f is trained only with respect to $\ell(\hat{y}_j)$. An excellent introduction to ML in general is (Shalev-Shwartz and Ben-David, 2014). Our theoretical framework includes the definition of an ML model

$$f: \mathbb{R}^{n \times n} \rightarrow \mathbb{R}^{n \times n}: \mathbf{A} \mapsto \mathbf{M}^{-1} \quad (5)$$

and the loss function

$$\ell(\mathbf{A}) := \kappa(\mathbf{A}f(\mathbf{A})) = \kappa(\mathbf{A}\mathbf{M}^{-1}). \quad (6)$$

The task of finding a preconditioner can now be formulated as an unsupervised learning problem. Given a size N training data set $\mathcal{T} = (\mathbf{A}_j)_{j=1}^N$ of SPD matrices the parameters of (5) are optimized with regard to (6) s. t.

$$\sum_{j=1}^N \ell(f(\mathbf{A}_j)) \rightarrow \min \quad (7)$$

employing a gradient-based optimization algorithm developed by Kingma and Ba (2014). So as not to be restricted by the spatial dimensions of input matrices we define the architecture of f as a so-called Convolutional Neural Network (CNN) which is a special class of ML models focusing on extracting local features in images via convolution operations (LeCun et al., 1989). In principle a CNN operates

the same way as the famous approach by Viola and Jones (2001) used for face detection in digital cameras. The only difference is that features in the CNN are trained on the data, rather than having to be constructed by hand in a meaningful way. The CNN architecture allows for f to come up with preconditioners for a wider range of SPD matrices since the model is invariant with respect to their shapes. The Parametric Rectified Linear Unit (PReLU)

$$\sigma: \mathbb{R} \rightarrow \mathbb{R}: x \mapsto \begin{cases} x & \text{if } x > 0 \\ ax & \text{otherwise} \end{cases}$$

where $a \in \mathbb{R}$ represents a trainable parameter, is chosen as the non-linear activation function in-between convolutional layers. Its advantage is that, unlike non-negative activations which crop each value to $[0, \infty)$, negative entries that might occur in the preconditioner M^{-1} can easily propagate through f .

When evaluating a convolutional layer with window size $k \times k$, $k > 1$ for a sparse image, additional non-zero elements are introduced due to the „bleeding“ effect demonstrated in Figure 1. Hence, the

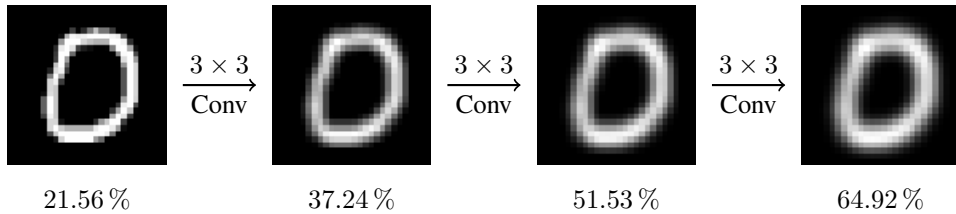


Figure 1: In a left-to-right order each convolution operation (Conv) with a 3×3 kernel further reduces the amount of zeros (black) thus increasing the density (below image) of the matrix. In order to not let this bleeding effect get out of hand our model only has four 2×2 convolutional layers.

amount of such layers in our CNN regulates the density of the learned preconditioner. We introduce merely four 2×2 convolution layers and since A is sparse, the sparsity of M^{-1} is preserved, resulting in a preconditioner that is cheap to apply. The two 1×1 convolution kernels do generate extra non-zeros. In Figure 2 a schematic representation of the CNN model is depicted.

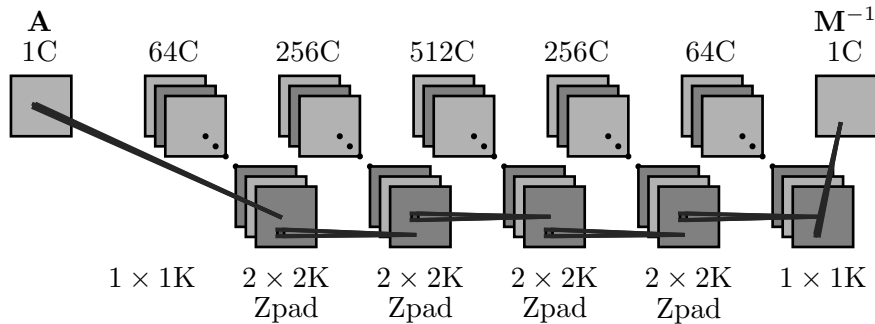


Figure 2: Standard fully convolutional six-layer CNN with 1×1 and 2×2 convolution kernels (K) stacked in an autoencoder-like structure of channels (C) sweeping over the matrix A resulting in a preconditioner M^{-1} . Due to this architecture A can be of arbitrary size. Parameters of this model are optimized according to (7). PReLU activations are employed in-between layers, zero padding (Zpad) preserves spatial dimensions.

The size of images CNNs have to process have initially been quite small, e. g., 28×28 pixels (LeCun et al., 1998). Only recently have researchers experimented with bigger images like 1024×1024 as well (Karras et al., 2017). Matrices A defining linear systems (1) exceed such dimensions by far and can cause a Graphics Processing Unit (GPU) used for training the model f to be out of memory. Since we are concerned with sparse SPD matrices, considerable computational power and memory allocated to saving training data T on the GPU would go to waste if sparsity is not properly exploited,

resulting among others in evaluation of the convolution kernels on large patches of zeros. Hence, we employ a custom CNN implementation based on PyTorch (Paszke et al., 2017), which is freely available on GitHub². Feeding the decomposition of \mathbf{A} into its strictly lower triangular part $\text{tril}(\mathbf{A})$ and diagonal $\text{diag}(\mathbf{A})$ to the CNN further reduces the computational burden, as seen in Figure 3.

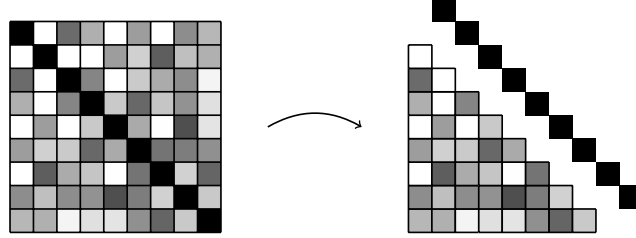


Figure 3: Instead of letting the CNN process the entire sparse SPD matrix \mathbf{A} (left) which can be quite large, only the strictly lower triangular part $\text{tril}(\mathbf{A})$ and diagonal $\text{diag}(\mathbf{A})$ (right) are used as input to reduce the computational burden. A custom CNN implementation exploits the sparsity of \mathbf{A} .

A Hermitian matrix \mathbf{H} is positive definite if and only if it has a unique Cholesky decomposition meaning there exists a unique lower triangular matrix \mathbf{T} with real and strictly positive diagonal elements s. t. $\mathbf{H} = \mathbf{T}\mathbf{T}^*$. Since the learned preconditioner needs to be SPD for PCG to work, such a unique decomposition has to exist for \mathbf{M}^{-1} as well. However, the output of the CNN model yields the strictly lower triangular part $\mathbf{T} := \text{tril}(f(\mathbf{A}))$ and the diagonal $\hat{\mathbf{D}} := \text{diag}(f(\mathbf{A}))$ which does not necessarily have only strictly positive elements. Only after pointwise application of a hard threshold $\mathbf{D} = \max\{\hat{\mathbf{D}}, \varepsilon\}$ with $\varepsilon = 10^{-3}$ is

$$\mathbf{M}^{-1} = (\mathbf{T} + \mathbf{D})(\mathbf{T} + \mathbf{D})^\top$$

guaranteed to be SPD.

Due to restrictions set by the PyTorch implementation the single-precision floating-point format is used for training data \mathcal{T} , model parameters and evaluation of f .

3 Results and Discussion

In this section we show the performance of our proposed preconditioning technique with ML based on solving the Pressure Poisson Equation (PPE) in a Computational Fluid Dynamics (CFD) simulation (Bridson, 2015) as well as characterizing the hydraulic state in pipe networks with flow continuity and headloss equations in EPANET 2 (Rossman, 2000).

Poisson's Equation

The incompressible Navier–Stokes equations describing the motion of viscous fluids read as

$$\begin{aligned} \partial_t \mathbf{u} + (\mathbf{u} \cdot \nabla) \mathbf{u} + \frac{1}{\rho} \nabla p &= \mathbf{F} + \nu \nabla^2 \mathbf{u}, \\ \nabla \cdot \mathbf{u} &= 0, \end{aligned}$$

where \mathbf{u} represents the fluid velocity vector field in \mathbb{R}^2 or \mathbb{R}^3 , ρ is the density of the fluid, p denotes the scalar pressure field, \mathbf{F} is the sum of external terms, and ν is the kinematic viscosity. To this day, existence and smoothness of Navier–Stokes solutions remain an open problem. Thus, various numerical schemes have been developed in the past in order to find satisfactory approximate solutions.

Typically, after some mathematical manipulations, as described in, e. g., (Chorin, 1967), enforcing incompressibility of the fluid leads to solving the so-called PPE given by

$$\nabla^2 p = \frac{\rho}{\Delta t} \nabla \cdot \mathbf{u}^*, \quad (8)$$

where \mathbf{u}^* is an intermediate solution.

²<https://github.com/traveller59/spconv>

Approximating the Laplacian ∇^2 in (8) with a finite-difference method in a Eulerian CFD simulation results in a large linear system

$$\mathbf{L}\mathbf{p} = \mathbf{d} \tag{9}$$

equal to (1). The matrix \mathbf{L} is sparse SPD, and \mathbf{d} corresponds to the right-hand side in (8). Note that, after a slight modification of the CNN f , our approach is also suited for particle-based CFD methods like Smoothed-Particle Hydrodynamics (SPH) originally developed by Gingold and Monaghan (1977). Two types of analytical preconditioners have already been applied to an incompressible SPH setup on GPUs by Chow et al. (2018).

Solving (9) and projecting \mathbf{u}^* onto the divergence-free subspace is generally the most expensive and time-consuming part of a fluid simulation (Tompson et al., 2016). In the following we state the results of increasing PCG performance for solving this large system of linear equations by applying our learned preconditioner \mathbf{M}^{-1} provided by the CNN f described in the previous section. In contrast to typical applications of ML where total system performance data is analyzed for learning purposes, we are aiming to lessen the computational burden of the numerical solution here.

The CNN is trained on 800 and validated on 200 occupancy grids of size 32×32 resulting in a 1024×1024 linear system (9). These are generated by intersecting an arbitrarily oriented 2D plane with two mutually exclusive sets of 3D models. We assume homogeneous Dirichlet boundary conditions in all our simulations generated with Mantaflow³. The geometry is given and fixed, thus our trained CNN needs to be evaluated only once for each CFD simulation which is achieved in constant time.

Training and validation of this model with a total of 1 180 934 internal parameters took 9.5 h on an NVIDIA Titan X GPU for 64 epochs, although it already converged at 40 epochs. The overall optimization progress is plotted in Figure 4. In Figure 5 we compare the residuals of analytical

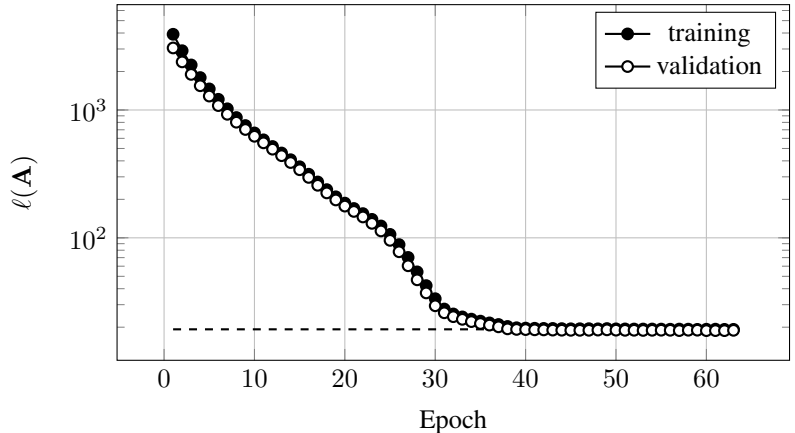


Figure 4: Semi-log plot of training and validation loss on 800 and 200 samples, respectively. The model converges to the empirical lower bound of about 19.25 (dashed line) which could be observed in several training runs. Note that the validation loss shows no signs of overfitting indicating good generalization properties of the model.

preconditioning approaches, such as Jacobi, incomplete Cholesky with zero-fill, and Algebraic MultiGrid (AMG), with our learned preconditioner. Clearly, the CNN is quite capable of designing \mathbf{M}^{-1} in such a way that PCG converges in less than half as much iterations. In Table 1 the quantitative results for PCG averaged over 200 samples not used for training can be observed. The time needed for constructing the preconditioners is negligible and has thus been ignored. Furthermore, it is important to note that once the CNN is evaluated we can reuse \mathbf{M}^{-1} in each time step whenever we need to solve (9) resulting in a linear increase of computation time saved as the simulation progresses.

In order to investigate the generalization capabilities of our model with respect to matrix dimensions we tested it on a 4096-dimensional problem and averaged over 80 samples. Even though it was originally trained on a small fluid domain it scales to bigger ones quite well, as can be seen in Table 2. The higher sparsity in comparison with an AMG approach causes each PCG iteration to be

³<http://mantaflow.com/>

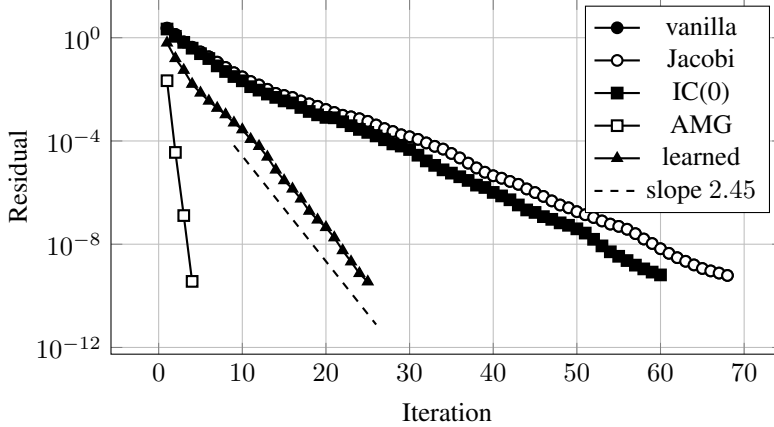


Figure 5: We consider a non-cherry-picked 4096-dimensional discrete Poisson problem and compare the residuals in a semi-log plot. Vanilla CG and Jacobi PCG can not be distinguished since they converge at the same speed, incomplete Cholesky with zero fill-in (IC(0)) is slightly better. Our preconditioner (learned) is 2.172% dense, converges with order 2.45, and outperforms the AMG approach in terms of runtime, cf. Table 2.

method	time [ms]	iter	κ	density
vanilla	9.829	54.64	139.367	–
jacobi	9.695	54.64	139.367	0.134 %
ic(0)	8.773	47.41	114.275	2.864 %
amg	3.082	4.02	1.261	98.686 %
learned	4.827	21.07	18.904	5.749 %

Table 1: Comparison of three standard preconditioning approaches with our learned ML model. The underlying problem is 1024-dimensional, all results are averaged over 200 samples. Since the size is so small all other preconditioners fail to beat the AMG approach in terms of runtime and iterations.

computationally more efficient and consequently faster.

EPANET 2

The open-source toolkit EPANET 2 (Rossman, 2000) developed by the U. S. Environmental Protection Agency is a software package for modeling pressure and flow conditions in a drinking water network. Assuming the network consists of n junction nodes a linear system (1) that reads as

$$\mathbf{A}\mathbf{h} = \mathbf{f},$$

where $\mathbf{A} \in \mathbb{R}^{n \times n}$ has to be solved for unknown nodal heads \mathbf{h} . It can be shown that \mathbf{A} is a real SPD matrix, thus suited for the PCG algorithm. Zecchin et al. (2012) found that AMG preconditioning

method	time [ms]	iter	κ	density
vanilla	22.70	98.15	472.727	–
jacobi	27.02	95.15	472.727	0.032 %
ic(0)	56.17	83.24	398.466	3.671 %
amg	52.02	4.72	1.539	99.471 %
learned	14.25	35.86	61.494	1.413 %

Table 2: Results for the same model that was used to generate Table 1, averaged over 80 samples. The 4096-dimensional problems here are four times as large as the ones in the training data. The high sparsity of our learned preconditioner induces considerable improvement in terms of runtime compared to all the other techniques.

outperforms the EPANET 2 solver if the networks are very large. Burger et al. (2015) accelerate the hydraulic simulations by utilizing a multicore capable solver but could not achieve satisfying results for networks with a real-world character.

We split a data set containing artificial water networks with a minimum of 1024 and up to 3971 junctions into 442 and 110 samples for training and testing, respectively. A revised version of the model employed for the PPE was used. Due to increased scattering of non-zero entries in \mathbf{A} the learned preconditioner is much more dense than it would be if \mathbf{A} resembled a band matrix resulting in slower evaluation of each PCG iteration. The overall results were inconclusive with even analytical preconditioning approaches failing in some cases. Special care is needed, e. g., reordering the input matrix to cluster non-zeros or adjusting the hyperparameters of the CNN model, which would be beyond the scope of this paper.

4 Conclusions

The rise of ML has mainly revolutionized image processing and data analysis techniques. We proposed applying these methods, namely a CNN, to solving large sparse systems of linear equations. However, the approximation error usually being introduced by ML approaches is undesirable in real-world engineering applications. By relying on the well-known iterative PCG algorithm we were able to utilize a CNN to design preconditioners, while still guaranteeing numerical accuracy of the obtained solutions. This novel approach has been found to work excellent for a variety of problems and in some instances even results in speed-up factors of about 2 to 3 for a single execution. We have been able to demonstrate the feasibility of our approach for the case study of CFD.

Despite the initial success, there still exist areas for continued development. Finding a replacement for the condition number computed via the costly Singular Value Decomposition (SVD) would accelerate the training process. We also intend to investigate learned preconditioning for more general types of equations not necessarily resulting in linear systems with SPD matrices.

Acknowledgments

We thank Gregor Burger for making his EPANET 2 code available. This research is part of the SPHAUL project 850738 which is funded by the Austrian Research Promotion Agency (FFG). We gratefully acknowledge the support of NVIDIA Corporation with the donation of two Titan X GPUs used for this publication.

References

- Benzi, M. (2002). Preconditioning Techniques for Large Linear Systems: A Survey. *Journal of Computational Physics*, 182(2):418–477.
- Bridson, R. (2015). *Fluid Simulation for Computer Graphics*. AK Peters/CRC Press.
- Burger, G., Sitzenfrei, R., Kleidorfer, M., and Rauch, W. (2015). Quest for a new solver for EPANET 2. *Journal of Water Resources Planning and Management*, 142(3):04015065.
- Chorin, A. J. (1967). A Numerical Method for Solving Incompressible Viscous Flow Problems. *Journal of Computational Physics*, 2(1):12–26.
- Chow, A. D., Rogers, B. D., Lind, S. J., and Stansby, P. K. (2018). Incompressible SPH (ISPH) with fast Poisson solver on a GPU. *Computer Physics Communications*, 226:81–103.
- Gingold, R. A. and Monaghan, J. J. (1977). Smoothed particle hydrodynamics: theory and application to non-spherical stars. *Monthly notices of the royal astronomical society*, 181(3):375–389.
- Karras, T., Aila, T., Laine, S., and Lehtinen, J. (2017). Progressive Growing of GANs for Improved Quality, Stability, and Variation. *arXiv e-prints*, page arXiv:1710.10196.
- Katrutsa, A., Daulbaev, T., and Oseledets, I. (2017). Deep Multigrid: learning prolongation and restriction matrices. *arXiv e-prints*, page arXiv:1711.03825.
- Kingma, D. P. and Ba, J. (2014). Adam: A Method for Stochastic Optimization. *arXiv e-prints*, page arXiv:1412.6980.

- LeCun, Y., Boser, B. E., Denker, J. S., Henderson, D., Howard, R. E., Hubbard, W. E., and Jackel, L. D. (1989). Backpropagation Applied to Handwritten Zip Code Recognition. *Neural Computation*, 1(4):541–551.
- LeCun, Y., Bottou, L., Bengio, Y., Haffner, P., et al. (1998). Gradient-based learning applied to document recognition. *Proceedings of the IEEE*, 86(11):2278–2324.
- Paszke, A., Gross, S., Chintala, S., Chanan, G., Yang, E., DeVito, Z., Lin, Z., Desmaison, A., Antiga, L., and Lerer, A. (2017). Automatic differentiation in PyTorch. *NIPS 2017*.
- Rossman, L. A. (2000). *EPANET 2: users manual*. US Environmental Protection Agency. Office of Research and Development.
- Saad, Y. (2003). *Iterative Methods for Sparse Linear Systems*. SIAM.
- Shalev-Shwartz, S. and Ben-David, S. (2014). *Understanding Machine Learning: From Theory to Algorithms*. Cambridge University Press.
- Tompson, J., Schlachter, K., Sprechmann, P., and Perlin, K. (2016). Accelerating Eulerian Fluid Simulation With Convolutional Networks. *arXiv e-prints*, page arXiv:1607.03597.
- Viola, P. and Jones, M. (2001). Rapid Object Detection using a Boosted Cascade of Simple Features. In *Proceedings of the 2001 IEEE Computer Society Conference on Computer Vision and Pattern Recognition (CVPR)*, pages 511–518.
- Zecchin, A. C., Thum, P., Simpson, A. R., and Tischendorf, C. (2012). Steady-State Behavior of Large Water Distribution Systems: Algebraic Multigrid Method for the Fast Solution of the Linear Step. *Journal of Water Resources Planning and Management*, 138(6):639–650.